

## The 7<sup>th</sup> Victor de Mello Goa Lecture: Climate resilient design of embankment using geocomposites

Rakshanda Showkat<sup>1#</sup> , G. L. Sivakumar Babu<sup>1</sup> 

Lecture

### Keywords

Intensity-Duration-Frequency curves  
Non-stationary Embankments  
Geocomposite  
Climate

### Abstract

Climate change is driving non-stationary rainfall patterns, intensifying both the frequency and magnitude of extreme precipitation events, which pose significant risks to earthen embankments. Traditional Intensity-Duration-Frequency (IDF) curves, based on stationary climate assumptions, often underestimate future hydrological loads. This study investigates the stability of embankments with and without geocomposite drainage layers under both stationary and non-stationary IDF scenarios, focusing on return periods of 10, 30, 50, and 100 years. Bengaluru, India, a monsoon-affected urban region, serves as the case study, with future rainfall projections derived from the CMIP6 SSP5-8.5 scenario to represent high-emission pathways. Numerical simulations reveal that unreinforced embankments under non-stationary conditions experience rapid pore-water pressure accumulation and a significant drop in Factor of Safety (*FOS*), reaching critical saturation in as little as 12 hours for 50-year return events. In contrast, geocomposite-reinforced embankments exhibit improved drainage, delayed saturation, and maintain *FOS* above 1.5 under stationary scenarios, and up to 18 hours of stability in the 100-year non-stationary case.

## 1. Introduction

The increasing frequency and intensity of extreme weather events pose significant challenges for infrastructure stability worldwide, especially in regions with pronounced seasonal rainfall. Among such events, heavy rainfall is particularly impactful, threatening the stability of geotechnical structures like embankments, retaining walls, and flood protection systems. These structures are often designed using Intensity-Duration-Frequency (IDF) curves, which estimate rainfall intensities based on historical data across various return periods (e.g., 10, 50, 100 years) and durations (e.g., hourly, daily). IDF curves are a fundamental design tool in hydrological engineering, enabling designers to establish capacity requirements and resilience thresholds for drainage and retention systems (Westra et al., 2014; Her et al., 2020).

Traditional IDF curves, however, assume stationarity—that is, they rely on the premise that historical climate conditions are indicative of future trends. This assumption is increasingly challenged by the evidence of climate change, which disrupts rainfall patterns, alters storm intensities, and increases the occurrence of extreme events beyond historical norms (IPCC, 2021). Recent studies show that rainfall intensity can increase by approximately 7% per degree Celsius rise in global temperature, indicating that IDF

curves based on stationary assumptions may not accurately capture the scale of future rainfall events (Knutson & Zeng, 2018; O’Gorman, 2015). This growing discrepancy between traditional design assumptions and emerging climate patterns necessitates the development of “non-stationary” IDF curves that incorporate climate projections, providing a more realistic basis for infrastructure planning and resilience (Cheng & AghaKouchak, 2014).

Monsoon-affected regions like Bengaluru, India, are particularly vulnerable to these changes. Projections indicate that such areas will experience not only increased annual rainfall but also shifts in seasonal intensity, leading to more frequent and intense short-duration events (Mishra et al., 2020a). Given these projections, the application of stationary IDFs in embankment and flood control system designs may result in underestimating future peak flows and, consequently, oversights in necessary structural capacity. Research reveals that embankments and drainage infrastructure designed with outdated stationary IDFs are at higher risk of saturation, slope failure, and erosion, particularly during unprecedented high-intensity events (Arnbjerg-Nielsen et al., 2013; Nguyen & Chen, 2021).

To address these issues, recent studies advocate for non-stationary IDF curves that incorporate climate model projections, thereby capturing anticipated changes in rainfall

#Corresponding author. E-mail address: rakshandashowkat07@gmail.com

<sup>1</sup>Indian Institute of Science, Department of Civil Engineering, Bengaluru, India.

Submitted on May 23, 2025; Final Acceptance on May 28, 2025; Discussion open until August 31, 2025.

Editor: Renato P. Cunha 

<https://doi.org/10.28927/SR.2025.008425>



This is an Open Access article distributed under the terms of the Creative Commons Attribution license (<https://creativecommons.org/licenses/by/4.0/>), which permits unrestricted use, distribution, and reproduction in any medium, provided the original work is properly cited.

intensity and frequency. By adjusting rainfall estimations to reflect anticipated climate variability, non-stationary IDF's provide a more accurate framework for designing infrastructure capable of withstanding future conditions. However, while non-stationary IDF's improve rainfall intensity predictions, the challenges posed by increased pore-water pressure and structural saturation remain significant for embankments. This brings to light another critical component in embankment design: the use of geosynthetic materials, specifically geocomposite layers.

Geocomposite layers, which consist of geotextiles and geonets, have proven effective in enhancing the drainage and stability of embankments during heavy rainfall events. They function both as capillary barriers, limiting water infiltration into deeper soil layers, and as drainage facilitators, allowing excess moisture to be redirected, thereby reducing pore-water pressures (Zornberg & Mitchell, 1994). In embankments and slopes, the integration of geocomposite layers has been shown to significantly delay critical saturation, maintain a higher Factor of Safety (*FOS*), and prevent early onset of slope failure, even under prolonged or intense rainfall conditions (Bahador et al., 2013; Her et al., 2018). These findings highlight the role of geocomposites as a valuable reinforcement technique in infrastructure subjected to high-intensity rainfall, particularly in scenarios where climate change is expected to exacerbate the frequency of extreme weather events.

Despite the increasing evidence of climate change impacts on rainfall intensity, there remains a critical gap in understanding how to best integrate non-stationary IDF's and geocomposite reinforcement in embankment design to ensure long-term stability. Existing studies have separately examined the benefits of non-stationary IDF's for hydrological design and geocomposites for soil stability; however, few have analyzed the combined effect of these innovations on embankment resilience under extreme future rainfall scenarios. This gap is particularly relevant for high-risk regions like Bengaluru, where non-stationary climate projections indicate substantial increases in peak rainfall intensities (IPCC, 2021; Mishra et al., 2020b). Without a combined approach, embankment designs may fail to fully address the complex interactions between increased rainfall intensity, pore-water pressure dynamics, and structural stability, leaving infrastructure susceptible to failure under future climate scenarios.

This study aims to bridge this research gap by evaluating embankments reinforced with geocomposite layers under both stationary and non-stationary IDF conditions, with a focus on rainfall return periods of 10, 30, 50, and 100 years. Using rainfall data from Bengaluru, India, and future projections from the CMIP6 SSP585 scenario, we simulate pore-water pressure distribution and Factor of Safety (*FOS*) in embankments with and without geocomposites. This approach allows for a comprehensive assessment of how geocomposite layers can enhance stability under extreme rainfall events anticipated by non-stationary IDF's. Ultimately, the research provides insights into adaptive design strategies that enhance the

resilience of embankments and other critical infrastructure in a changing climate, emphasizing the need for climate-informed IDF modelling and geosynthetic reinforcement to ensure safe and sustainable infrastructure.

## 2. Background and literature review

### 2.1 Intensity-duration-frequency (IDF) curves

IDF curves are statistical representations used to estimate the intensity of rainfall events of various durations (e.g., hourly, daily) and return periods (e.g., 10, 50, or 100 years). These curves are crucial for engineering applications, especially for designing flood control systems, embankments, and other drainage infrastructures (Her et al., 2018). Traditional IDF curves assume that rainfall patterns observed in historical data will continue unchanged into the future, making them “stationary.” However, numerous studies have demonstrated that climate change introduces significant non-stationarity into precipitation patterns, leading to the need for updated, non-stationary IDF curves (Her et al., 2020).

### 2.2 Impact of climate change on rainfall

Climate change is expected to increase the intensity and frequency of extreme weather events. Projections from General Circulation Models (GCMs) indicate a rise in global temperatures and subsequent changes in hydrological cycles, resulting in more intense and frequent rainfall in many regions (IPCC, 2021). In the Indian context, cities like Bengaluru are expected to experience increased annual rainfall, further complicating drainage, and flood management efforts (Mishra et al., 2020a).

The implications of these changes for infrastructure design are profound. The use of outdated, stationary IDF curves could lead to under-designed drainage systems, resulting in frequent failures or oversizing that is economically inefficient. Non-stationary IDF curves that incorporate climate model projections offer a more accurate representation of future conditions. If rainfall changes over time due to climate change, the curves may provide an insufficient estimate (or an excessive estimate) of future rainfall intensities or depths. Thus, their use could result in under-designed (or overdesigned) engineering projects. However, climate change is an evolving science and forecasting how rainfall patterns and IDF's will change in response to it remains an imprecise analysis.

Scaling IDF curves using projected future rainfall from global climate models (or a general circulation model) (Her et al., 2020) is an appealing alternative because changes seen in rainfall from the model output between historical and future periods should theoretically include both the changes caused by temperature as well as other aspects of weather patterns that may influence rainfall intensity in a given location.

Projections from the General Circulation Models (GCMs) play a vital role in understanding the future changes in climate. However, spatial resolution at which GCMs are run is often too coarse to get reliable projections at the regional and local scale. Precipitation projections at higher spatial resolution are required for the climate impact assessments. Moreover, precipitation from the GCMs have a bias due to their coarse resolution or model parameterizations. Therefore, for the assessment of the climate change and its impacts on different sectors (e.g., water resources, agriculture), bias-correction is required. Both statistical and dynamical approaches are used for downscaling and bias correction of climate change projections from GCMs. Statistical approaches are based on the distribution and relationship between the observed and projected data for the historical period. On the other hand, dynamical downscaling approaches are based on regional climate model forced with the boundary conditions from the coarse resolution GCMs. Both statistical and dynamical downscaling approaches have limitations. The primary limitation of the dynamical downscaling is related to the requirement of computational efforts to run the regional climate models at higher spatial and temporal resolution. Moreover, dynamical downscaling may not remove the bias in climate variables, which might require corrections based on the statistical approaches. Given these limitations, statistical bias correction approaches are widely used in climate change impact assessments.

### 2.3 Geocomposite layers in embankment design

Geocomposite layers consist of geotextiles and geonets that are used to manage water flow in embankments. These layers enhance the drainage capabilities of the soil, acting as both a capillary barrier to prevent rapid infiltration and as a drainage layer that facilitates water flow out of the embankment. The inclusion of geocomposites is particularly beneficial in regions experiencing heavy rainfall or in embankments subjected to prolonged periods of saturation (Zornberg & Mitchell, 1994).

Previous studies have shown that geocomposite layers can significantly improve embankment stability by reducing pore-water pressure and maintaining the soil's shear strength (Bahador et al., 2013). This study will extend this research by simulating the effects of geocomposite layers under different rainfall return periods using both stationary and non-stationary IDF curves.

## 3. Methodology

### 3.1 Study area and data collection

The study focuses on Bengaluru, India, a region characterized by monsoonal rainfall patterns. The city receives an average annual rainfall of approximately 931 mm,

distributed over 60 rainy days. Historical daily precipitation data from the India Meteorological Department (IMD) for the period 1951–2015 was used to develop the stationary IDF curves. Climate projections were sourced from five Global Circulation Models (GCMs) under the CMIP6 framework, using the SSP585 scenario, which assumes high greenhouse gas emissions until the end of the 21st century.

### 3.2 IDF curve development

Two sets of IDF curves were developed for this study: stationary and non-stationary. The stationary IDF curves were based on historical rainfall data and represent the traditional design approach. Non-stationary IDF curves were developed using rainfall projections from GCMs for the 2071–2100 period. These projections account for the expected increase in rainfall intensity due to climate change. Daily precipitation at 0.25° can be obtained from the India Meteorological Department (IMD) for the Indian region. Pai et al. (2014) developed gridded daily precipitation for India using station observations from more than 6000 stations located across India. The precipitation captures critical features of the Indian summer monsoon, including higher rainfall in the Western Ghats and northeastern India and lower rainfall in the semi-arid and arid regions of western India. Besides, gridded precipitation captures the orographic rain in the Western Ghats and foothills of Himalaya. The gridded precipitation data from IMD has been used for various hydroclimatic applications. Use gridded observations for bias correction as station data are not available. Outputs ( $x_m$ ) from 5 CMIP6-GCMs can be used, which are available at different resolutions. Observations for the variable at the resolution of 0.25-degree are obtained from the IMD, for Indian Region.

Precipitations from CMIP6-GCMs are available at different spatial resolutions (Mishra et al. 2020b). For instance, the spatial resolution of the CMIP6 projection varies from 0.7° (EC-Earth3) to more than 2° (CanESM5). Mapped transformation to bias corrects the outputs for the historical period can be done and the SSP585 scenarios for the 100 years period for the precipitation scenarios can be used under r1i1p1f1 initial condition at daily time scale. The scenarios used in the CMIP6 combine Shared Socioeconomic Pathways (SSP) and target radiative forcing levels at the end of the 21st century. Regrid the precipitation data from CMIP6 to 1° spatial resolution to make them consistent. However, the effect of regridding using bilinear interpolation was checked by comparing the gridded datasets against the raw data for all-India mean of precipitation. We did not find any considerable differences in the all-India averaged precipitation and temperature using regridded and raw output from the GCMs.

The average annual rainfall depth for Bengaluru city is 931 mm, spread across 60 rainy days in a year (Ramachandra & Mujumdar, 2009). The stationary and non-stationary IDF

curve for Bengaluru for a return period of 10, 30, 50 and 100 years is shown in Figure 1 and 2, developed utilizing the hourly data from IMD’s daily gridded (Pai et al., 2014) data at a spatial resolution of for a period of 100 years. The data is disaggregated for durations less than 1 h and various return period by using Equation 1, which is the most common rainfall disaggregation model of IDF relationship applicable to most of the geographical locations.

$$I(mm/hr) = A*(t+t_0)^B \tag{1}$$

where  $I$  is the intensity of rainfall,  $A$ ,  $B$  and  $t_0$  represent the coefficients for each return period ( $T$ ) in years,  $t$  is the duration of precipitation in hours. Tables 1 and 2 show the coefficient of precipitation for stationary and non-stationary IDF.

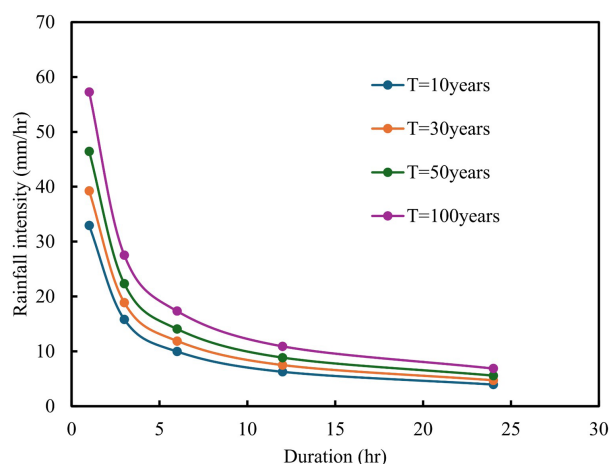


Figure 1. Stationary IDF for Bengaluru.

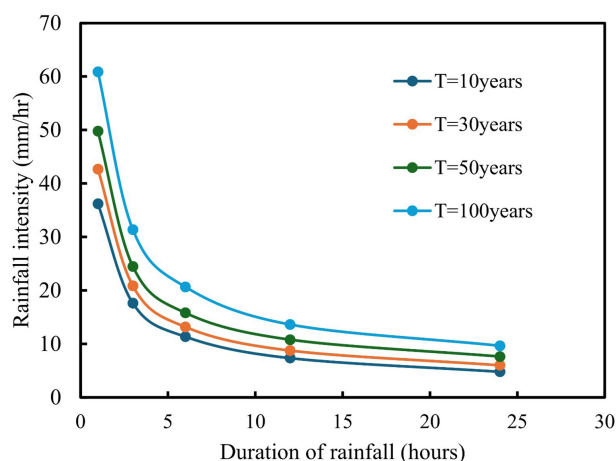


Figure 2. Nonstationary IDF for Bengaluru.

### 3.3 Embankment model and geocomposite layer simulation

The embankment model was developed using a finite difference method (FEM) simulation to evaluate pore-water pressure distribution and  $FOS$  under varying rainfall intensities. Two scenarios were considered:

- An embankment without a geocomposite layer.
- An embankment with a geocomposite layer consisting of a geotextile and a geonet.

The hydraulic properties of the geocomposite were based on experimental data from Gofar & Min Lee (2008), which showed high drainage efficiency and moisture retention capacity. The embankment was subjected to a continuous 24-hour rainfall simulation for each return period.

To represent the variation of suction and effective saturation in the embankment upon rainfall, Van-Genuchten (1980) model was used to present a relation between volumetric water content  $\theta$  and suction  $s$  as given in Equation 2.

$$\theta = \frac{1}{\left[1 + \left(\frac{s}{\alpha}\right)^{n_e}\right]^m} \tag{2}$$

where inverse of  $\alpha$  corresponds to the air entry value,  $n_e = 1 - 1/m$  and  $m$  are the fitting parameters. In terms of non-dimensional form,  $\theta$  can be expressed as:

$$\theta = \frac{\theta - \theta_r}{\theta_s - \theta_r} \tag{3}$$

where  $\theta$  represents the volumetric water content at a given suction, maximum and residual water contents are represented

Table 1. Coefficients for stationary IDF.

T (years)	Coefficient A	Coefficient B	Coefficient $t_0$
10	35.8	-0.795	0.1034
30	46.7	-0.813	0.112
50	58.0	-0.857	0.124
100	63.8	-0.882	0.128

Table 2. Coefficients for Non- stationary IDF.

T (years)	Coefficient A	Coefficient B	Coefficient $t_0$
10	36.1	-0.745	0.1124
30	47.2	-0.803	0.120
50	58.4	-0.827	0.131
100	64.5	-0.842	0.136

by  $\theta_s$  and  $\theta_r$ , respectively. The parameter  $\theta_s$  corresponds to zero suction condition obtained by extrapolating the SWCC,  $\theta_r$  represents the residual suction condition and lies below the air-entry value and  $\alpha$  represents the inverse of air-entry value.

A range of parameters, detailed in Table 3, was employed to determine the Soil Water Characteristic Curve (SWCC) for both the embankment soil and the geocomposite layer. Although the Barcelona Basic Model (BBM) parameters for the embankment soil were adopted to represent Kaolin, due to limited available data, the SWCC and hydraulic conductivity inputs were sourced from experimental findings on Kaolin soil presented by Gofar & Min Lee (2008) as shown in Figure 3 and 4. The geocomposite layer, consisting of a geonet core flanked by two geotextile layers, was characterized using SWCC and hydraulic conductivity curves, as illustrated in Figures 3 and 4 (Bahador et al., 2013). The geocomposite exhibited a steeper SWCC and higher air entry values (*AEV*) for both geotextile and geonet components relative to soil, which induces increased suction below the interface and reduced suction above it due to water accumulation (Bahador, 2012). These hydraulic properties enable the geocomposite to function effectively as both a drainage medium and a capillary barrier (Zornberg & Mitchell, 1994). In FLAC modelling, the geocomposite's drainage function was simulated by assigning zero pore pressure at specified nodes, while its mechanical behaviour was represented using a linear elastic model with an elastic modulus of  $1.18 \times 10^3$  MPa and Poisson's ratio of 0.1 (Bahador et al., 2013). The BBM framework also incorporates shear modulus for geocomposite elasticity, with sensitivity analyses indicating that variations in modulus influence the resulting displacement fields.

In this study, a nonwoven geocomposite layer was incorporated to function as a drainage layer within an embankment undergoing infiltration, as illustrated in Figure 5.

## 4. Results

### 4.1 Pore-water pressure distribution using stationary IDF curves

In the case of embankments constructed without the inclusion of geocomposite drainage layers, simulations

conducted under stationary Intensity-Duration-Frequency (IDF) conditions representative of historical precipitation data without accounting for future climatic variability revealed a consistent and progressive accumulation of pore-water pressure throughout the embankment body across all analysed return periods: 10, 30, 50, and 100 years. Under relatively lower return periods (10-year and 30-year events),

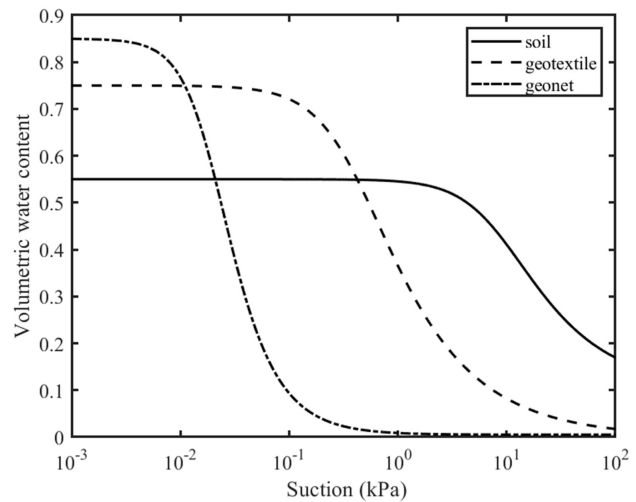


Figure 3. SWCC of soil and geocomposite layer.

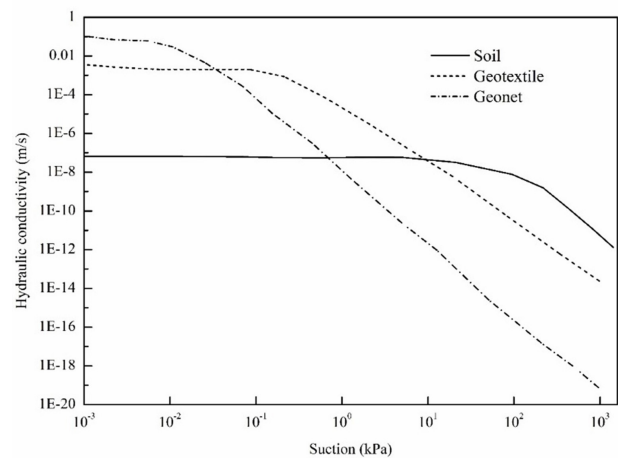


Figure 4. Hydraulic conductivity curves.

Table 3. Hydraulic properties of soil and geocomposite.

Materials	$\theta_s$	$\theta_r$	$\alpha$ (1/kPa)	$n_e$	$k_{sat}$ (m/s)
Embankment soil (Gofar & Min Lee, 2008)	0.6	0.1	0.014	1.33	$6.8 \times 10^{-8}$
Geotextile layer (Stormont et al., 2001)	0.75	0	2.577	1.68	$2.89 \times 10^{-3}$
Geonet (Ramos, 2001)	0.85	0.005	50.251	2.19	$1 \times 10^{-1}$

the increase in pore-water pressure was moderate. Saturation predominantly occurred within the upper soil horizons due to limited rainfall intensity and duration, as evidenced by the pore-pressure contour distributions in Figure 6a-d. During these lower-magnitude events, the embankment structure exhibited sufficient resilience, with the Factor of Safety (*FOS*) remaining above critical thresholds. Specifically, stability was maintained up to 18 hours in the 10-year return period

scenario and up to approximately 12 hours in the 30-year case before signs of mechanical compromise emerged.

However, under higher-magnitude return periods (50-year and 100-year events), the embankment experienced significantly more adverse hydraulic conditions. The simulated pore-water pressure rose rapidly and penetrated into deeper soil layers, driven by prolonged rainfall infiltration. In the 100-year return period scenario, by the 18-hour mark, nearly the entire

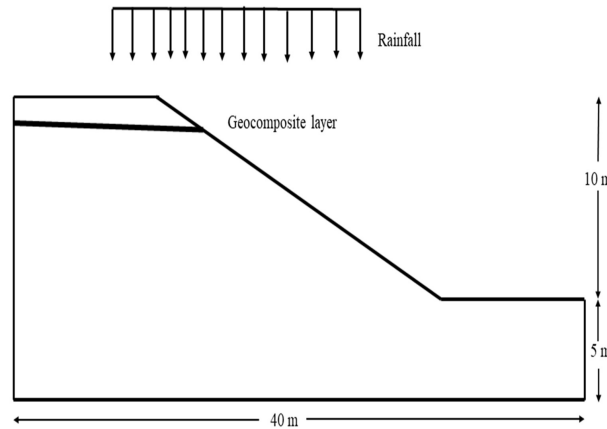


**Figure 5.** Geometry of embankment with geocomposite layer.

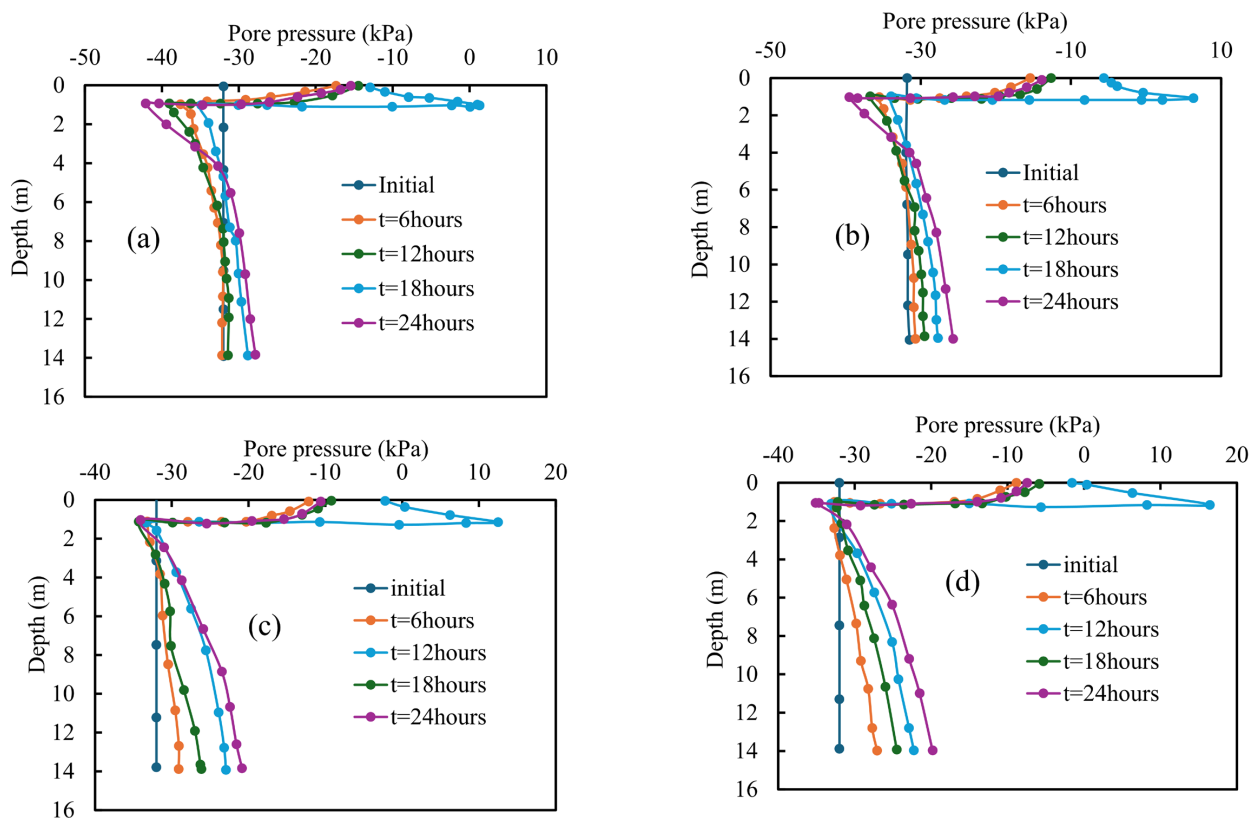


**Figure 6.** Pore pressure distribution in embankment with geocomposite with: (a) 10 years return period, (b) with 30 years return period, (c) 50 years return period, and (d) 100 years return period.

embankment cross-section exhibited high saturation levels. This hydraulic loading condition induced a substantial loss in matric suction, leading to a marked decline in the effective stress state of the soil matrix. As a result, the *FOS* deteriorated sharply, approaching failure thresholds ( $FOS \approx 1.0$ ) within 24 hours, thus indicating a high probability of structural failure under such extreme yet increasingly probable rainfall events.

In contrast, embankments that incorporated geocomposite layers demonstrated a markedly different hydraulic and mechanical response under identical stationary IDF scenarios. The geocomposite system, composed of a geonet core enclosed between two geotextile sheets, initially acted as a capillary barrier. Due to its high air entry value (*AEV*) and steep Soil Water Characteristic Curve (SWCC), it effectively delayed the downward migration of moisture during the early stages of rainfall infiltration. This barrier effect mitigated the rate of pore-water pressure build-up, particularly within the lower embankment layers, during the critical early hours of the rainfall event. This control was evident across all return periods, with the geocomposite substantially reducing moisture ingress and suction loss during the first 12 hours.

As rainfall persisted, the geocomposite's drainage function became dominant. The permeable structure facilitated lateral and vertical redistribution of water, thus promoting dissipation of excess pore pressure and preserving unsaturated conditions within a significant portion of the soil profile. This dual behaviour capillary hindrance followed by enhanced drainage proved highly effective in maintaining mechanical stability. Notably, even under the 100-year return period scenario, the embankment with geocomposite layers maintained a *FOS* greater than 1.5 after 24 hours of continuous rainfall. This indicates that the presence of the geocomposite significantly extends the critical response time and enhances the overall hydraulic performance and mechanical resilience of the embankment structure under extreme precipitation loading conditions.

#### 4.2 Pore-water pressure distribution using non-stationary IDF curves

Under non-stationary Intensity-Duration-Frequency (IDF) scenarios—derived from future climate projections incorporating anthropogenic warming effects and increased atmospheric moisture content the embankment response exhibited markedly accelerated hydraulic loading, particularly at higher return periods (50- and 100-year events). These curves account for the non-linearity and temporal evolution of extreme rainfall intensity due to climate change, resulting in steeper rainfall hyetographs and higher cumulative precipitation volumes over shorter durations. In embankments constructed without geocomposite reinforcement, this translated into a significantly more aggressive rate of pore-water pressure development. Saturation thresholds were reached substantially earlier compared to stationary cases: within approximately 12 hours for the 50-year return period and as early as 8 hours

for the 100-year scenario, as evidenced in Figure 6a-d. The rapid infiltration under high rainfall intensities induced immediate loss of matric suction and led to a pronounced hydraulic gradient, causing moisture fronts to advance swiftly into the lower embankment strata.

This expedited hydraulic loading reduced effective stress and initiated a sharp decline in the Factor of Safety (*FOS*). For the 100-year non-stationary event, the embankment approached incipient failure conditions within 18 hours of rainfall onset, demonstrating a critical reduction in mechanical stability due to the elevated saturation profile and diminished shear strength of the soil matrix. The vertical propagation of pore pressure fronts under non-stationary rainfall exceeded the rates observed in stationary conditions by over 50%, confirming the inadequacy of legacy IDF-based designs under evolving climate regimes.

Conversely, embankments incorporating geocomposite layers exhibited an improved but not invulnerable response to non-stationary forcing. The geocomposite system, through its capillary barrier effect and enhanced in-plane transmissivity, effectively moderated the upward migration of pore pressure, and facilitated lateral water dispersion. During the initial phase of rainfall exposure (first 12–15 hours), the geocomposite delayed the saturation of deeper layers and maintained lower suction gradients across the soil profile. However, the elevated rainfall intensities characteristic of non-stationary IDF curves still resulted in accelerated hydraulic loading compared to the stationary case. For the 100-year return period, while the presence of the geocomposite ensured that *FOS* remained above the stability threshold of 1.0 up to approximately 18 hours, the system approached hydraulic saturation by the 24-hour mark.

This temporal extension of structural integrity illustrates the functional resilience of the geocomposite under severe climatic stressors, though it also underscores the limitations of passive drainage systems under sustained extreme hydrological inputs. Ultimately, the geocomposite layer served as a critical mitigation component, but its effectiveness diminishes under long-duration, high-magnitude precipitation events anticipated by non-stationary projections, necessitating further optimization of embankment designs for future climate resilience.

#### 4.3 Effects of stationary and non-stationary IDF curves

The analysis was extended to consider the effects of using stationary versus non-stationary IDF curves for modelling rainfall intensities. Stationary IDF curves, which assume historical rainfall patterns remain constant over time, provide a simplified approach. However, as climate change impacts intensify, this assumption can result in an underestimation of future rainfall intensity and frequency, potentially leading to unsafe embankment designs.

When stationary IDF curves were applied, pore-water pressure distributions showed slower but steady increases with rainfall duration across all return periods. For instance,

after 6 hours of rainfall under a 50-year return period, the pore-water pressure remained moderate, and the *FOS* did not drop significantly. However, as rainfall persisted beyond 18 hours, particularly under the 100-year return period, the embankment reached critical saturation levels quicker, indicating a potential failure if the geocomposite layer were absent.

In contrast, using non-stationary IDF curves which account for the projected increase in rainfall intensity due to climate change produced more aggressive pore-water pressure rises, especially in the 50- and 100-year scenarios. Non-stationary IDF curves reflect the dynamic and changing nature of rainfall, particularly in regions like Bengaluru, where future climate projections indicate higher rainfall intensities. As a result, embankments experienced more rapid saturation and higher pore pressures under these conditions. However, the inclusion of the geocomposite layer significantly mitigated these impacts by accelerating drainage and preventing dangerous levels of saturation, even as rainfall intensities increased.

The most dramatic difference between stationary and non-stationary IDF applications was observed during the higher return period events (100 years). Under non-stationary conditions, without geocomposites, the embankment would experience critical pore pressures and fail earlier, as the system would not account for future increases in intensity. The geocomposite proved essential in prolonging the time to failure by reducing saturation rates and maintaining a higher *FOS*, even in extreme rainfall events.

#### 4.4 Factor of safety (*FOS*) comparison across return periods and IDF types

The *FOS* analysis demonstrated notable differences in embankment stability under stationary versus non-stationary

IDF curves, especially in embankments without geocomposite layers as shown in Figure 7a. Under stationary IDF conditions, the *FOS* remained stable across all return periods up to 12 hours but dropped to near failure levels in the 50- and 100-year return periods by the 18-hour mark. In contrast, non-stationary IDF conditions caused a steep decline in *FOS* within the first 12 hours, with failure thresholds reached much sooner for higher return periods, particularly in the absence of geocomposites as shown in Figure 7b.

For embankments reinforced with geocomposite layers, the *FOS* values remained consistently higher across all return periods in both stationary and non-stationary scenarios. The geocomposite layer significantly prolonged stability, keeping *FOS* values above 1.5 for most of the 10- and 30-year return periods and extending stability to 18 hours in the 100-year scenario under non-stationary IDF curves. This suggests that geocomposites are crucial in maintaining embankment stability under extreme future rainfall scenarios.

The *FOS* behaviour across different return periods (10, 30, 50, and 100 years) further highlighted the role of geocomposite layers. For lower return periods (e.g., 10 years), the *FOS* remained high, reflecting the embankment's resilience to short-duration, moderate-intensity rainfall. The geocomposite layer delayed saturation and enabled drainage before critical shear strength reductions occurred. For higher return periods (50 and 100 years), the *FOS* decreased more significantly, particularly under non-stationary IDF curves, where the rainfall intensity was higher than historical norms. However, the geocomposite layer consistently maintained a safer *FOS* by enabling excess water to be efficiently drained and preventing the rapid buildup of pore pressure.

Without the geocomposite layer, embankments subjected to non-stationary IDF curve scenarios would experience a catastrophic reduction in *FOS* during long return periods, often approaching failure thresholds ( $FOS = 1$ ). This finding

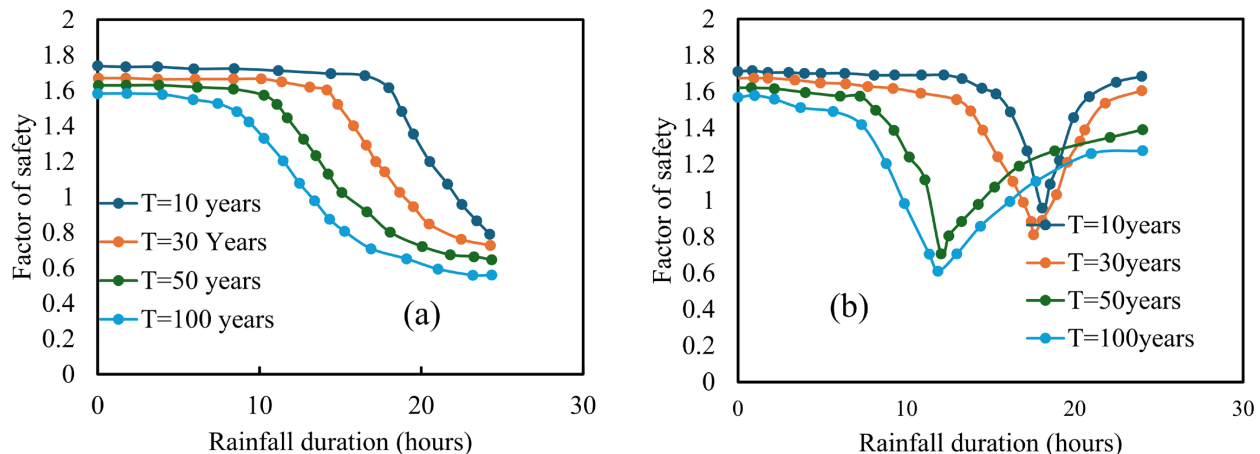


**Figure 7.** Variation of *FOS* of embankment: (a) at various return periods, and (b) with geocomposite at various return periods.

underscores the importance of factoring in non-stationary IDF's when designing embankments to withstand future climate variability.

#### 4.5 Flux rate calculations

The computed flux rates at the crest of the embankment, as illustrated in Figure 8, reveal a dynamic evolution of infiltration behaviour under transient hydrological loading. Initially, the flux rate exhibited a gradual decline over time, characteristic of decreasing hydraulic gradients as the surface layers approached saturation. This behaviour is consistent with classic infiltration theory, wherein matric suction decreases near the surface with prolonged wetting, reducing the capillary-driven flow component.

A pronounced inflection point in the flux rate curve was observed when the advancing wetting front intersected the geotextile component of the geocomposite system. At this interface, a sudden reduction in vertical flux was recorded, indicating the onset of capillary barrier effects induced by the contrast in pore-size distribution between the embankment soil and the geotextile. This phenomenon is analogous to the mechanism described by Miller & Gardner (1962) in their seminal study on vertical flow through layered soil columns, where a fine-over-coarse stratification imposes a temporary impedance to flow due to higher air entry values in the underlying coarser medium.

Post-intersection, the flux rate stabilized at a lower magnitude, indicative of a redistribution regime dominated by lateral drainage along the plane of the geonet core. The geocomposite's internal transmissivity allowed for rapid in-plane flow, effectively diverting infiltrating water away from the vertical percolation path and mitigating pore pressure accumulation in the underlying soil matrix. This behaviour underscores the drainage capacity of geocomposite systems: by combining high in-plane hydraulic conductivity with capillary tension modulation, geocomposites serve

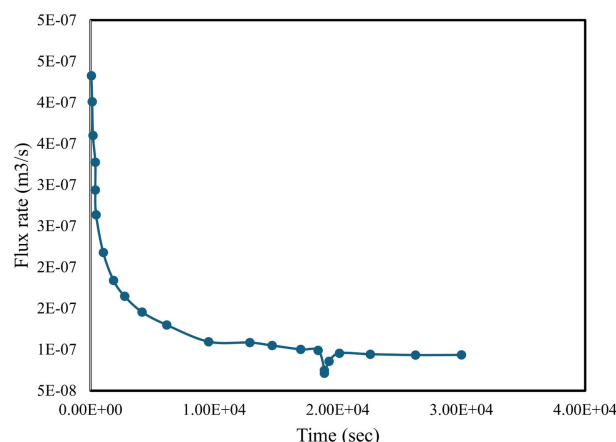


**Figure 8.** Flux rate with time.

both to delay vertical saturation and to provide preferential drainage pathways.

Quantitatively, the observed drop in flux magnitude corresponds to the initiation of water storage above the geotextile until the matric potential of the overlying soil exceeds the air-entry pressure of the geotextile. Once this threshold is overcome, vertical flow resumes, albeit at a reduced rate due to redistribution through the geonet. The interplay between capillary forces and hydraulic conductivity within the geocomposite is critical in controlling the timing and magnitude of subsurface saturation, thereby directly influencing the overall hydraulic response and stability of the embankment system under intense rainfall events.

## 5. Discussion

### 5.1 Impact of stationary vs. non-stationary IDF curves on embankment stability

The results underscore the limitations of using stationary IDF curves, which rely solely on historical rainfall data. While stationary IDF's can provide reasonable estimates for current rainfall patterns, they do not account for the projected intensification of rainfall events due to climate change. Consequently, designs based on stationary IDF's may underestimate future rainfall intensities, especially for higher return periods (50 and 100 years). This underestimation increases the risk of embankment failure, as observed in the steep declines in *FOS* values under simulated non-stationary IDF conditions. In contrast, non-stationary IDF curves provide a more realistic estimate of future rainfall intensities, especially in climate-sensitive regions like Bengaluru, where rainfall patterns are projected to intensify over the coming decades.

In embankments without geocomposite layers, the non-stationary IDF conditions led to rapid soil saturation and a critical drop in *FOS* within hours. This suggests that traditional embankment designs, relying on stationary IDF's, may not be sufficient for future climate scenarios. The findings align with recent research emphasizing the need to incorporate non-stationary IDF's in infrastructure planning, especially for long-term resilience (IPCC, 2021).

### 5.2 Role of geocomposite layers in enhancing embankment stability

The incorporation of geocomposite layers significantly improves embankment stability, as demonstrated by the higher *FOS* values across all scenarios. Geocomposite layers provide dual functionality as capillary barriers and drainage facilitators. Initially, they act as moisture barriers, preventing the rapid infiltration of water into deeper soil layers. As rainfall continues, they transition to a drainage function, allowing excess moisture to be directed away from the embankment, thereby reducing pore pressure, and enhancing stability.

The results from this study show that embankments with geocomposite layers maintain higher *FOS* values, even under the extreme conditions simulated by non-stationary IDF curves. This supports previous findings by Bahador et al. (2013) and Zornberg and Mitchell (1994), which highlighted the effectiveness of geocomposites in enhancing stability in saturated soils. Specifically, the presence of geocomposites delayed critical saturation by up to 6 hours in the 50- and 100-year return periods, indicating that geocomposites provide critical time margins for embankment resilience during prolonged rainfall.

### 5.3 Implications for infrastructure design under changing climate conditions

The findings suggest that infrastructure design should prioritize the integration of both non-stationary IDF curves and geocomposite layers to accommodate future climate scenarios effectively. Non-stationary IDF curves provide a realistic assessment of future rainfall intensities, which are essential for the accurate estimation of pore pressure and *FOS*. By using non-stationary IDFs, engineers can design embankments that are resilient to future climate variability, thereby reducing the likelihood of failure.

Geocomposite layers emerge as a highly effective means of mitigating the effects of increased rainfall intensity on embankment stability. Their ability to control pore-water pressure distribution and delay saturation under extreme rainfall makes them particularly valuable in regions prone to heavy monsoons and climate-induced rainfall intensification. This study's results align with broader research indicating that geosynthetics, when used in tandem with climate-adaptive IDF models, enhance the resilience of critical infrastructure (Her et al., 2018; Oguz et al., 2024).

## 6. Conclusions

This study demonstrates the critical need for climate-adaptive strategies in embankment design, emphasizing the limitations of traditional, stationary Intensity-Duration-Frequency (IDF) curves under evolving climate conditions. The findings show that embankments without geocomposite layers exhibit rapid pore-water pressure increases and significant reductions in the Factor of Safety (*FOS*) under non-stationary IDF conditions, with failure thresholds reached much faster in high return periods, such as the 50- and 100-year events. Conversely, the integration of geocomposite layers within embankments proves highly effective in moderating pore pressures, delaying critical saturation, and sustaining higher *FOS* values across all return periods. Specifically, under the 100-year return period with non-stationary conditions, embankments reinforced with geocomposites maintain stability up to 18 hours longer than their unreinforced counterparts. These results underscore two key recommendations for future embankment design:

- Incorporate Non-Stationary IDF Curves: Accounting for projected climate-induced changes in rainfall patterns provides a more accurate basis for infrastructure planning, mitigating under-design risks associated with outdated stationary models;
- Utilize Geocomposite Reinforcements: Geocomposite layers enhance resilience by acting as both drainage facilitators and capillary barriers, significantly extending the time to saturation and improving overall stability during extreme rainfall events.

## Declaration of interest

The authors declare that they have no known competing financial interests or personal relationships that could have appeared to influence the work reported in this paper.

## Authors' contributions

Rakshanda Showkat: software, formal analysis, data curation, investigation, methodology, visualization, validation, writing – original draft, conceptualization. G L Sivakumar Babu: writing – review & editing, project supervision.

## Data availability

The datasets generated analyzed in the course of the current study are available from the corresponding author upon request.

## Declaration of use of generative artificial intelligence

This work was prepared without the assistance of any generative artificial intelligence (GenAI) tools or services. All aspects of the manuscript were developed solely by the authors, who take full responsibility for the content of this publication.

## List of symbols and abbreviations

$k_{sat}$	Saturated permeability
$m$	fitting parameter
$n_e$	fitting parameter
$s$	Matric suction
$t_0$	coefficient for each return period
$t$	Duration of precipitation in hours
$x_m$	Outputs
$A$	coefficient for each return period
$B$	coefficient for each return period
$AEV$	air entry value
BBM	Barcelona Basic Model
$FOS$	Factor of safety



GCM	General Circulation Model
$I$	Intensity of rainfall
IDF	Intensity-Duration-Frequency
SWCC	Soil Water Characteristic Curve
$\alpha$	Air entry value
$\theta$	Volumetric water content
$\theta_r$	Residual water content
$\theta_s$	Maximum water content

## References

- Arnbjerg-Nielsen, K., Willems, P., Olsson, J., Beecham, S., Pathirana, A., Bülow Gregersen, I., Madsen, H., & Nguyen, V.T. (2013). Impacts of climate change on rainfall extremes and urban drainage systems: a review. *Water Science and Technology*, 68(1), 16-28. PMID:23823535. <http://doi.org/10.2166/wst.2013.251>.
- Bahador, M. (2012). *Thermal, hydraulic, and mechanical response of unbound pavement layers with geosynthetics at the subgrade-base course interface*. [PhD thesis, North Carolina State University]. North Carolina State University.
- Bahador, M., Evans, T.M., & Gabr, M.A. (2013). Modeling effect of geocomposite drainage layers on moisture distribution and plastic deformation of road sections. *Journal of Geotechnical and Geoenvironmental Engineering*, 139(9), 1407-1418. [http://dx.doi.org/10.1061/\(ASCE\)GT.1943-5606.0000877](http://dx.doi.org/10.1061/(ASCE)GT.1943-5606.0000877).
- Cheng, L., & AghaKouchak, A. (2014). Nonstationary precipitation intensity-duration-frequency curves for infrastructure design in a changing climate. *Scientific Reports*, 4, 7093. PMID:25403227. <http://doi.org/10.1038/srep07093>.
- Gofar, N., & Min Lee, L. (2008). Extreme rainfall characteristics for surface slope stability in the Malaysian Peninsular. *Georisk*, 2(2), 65-78. <http://doi.org/10.1080/17499510802072991>.
- Her, Y.G., Brym, Z., Smyth, A., & Bassil, E. (2020). How is our future climate projected? AE546/AE546, 11/2020. *Agricultural and Biological Engineering*, 2020(6), 1-5. <http://doi.org/10.32473/edis-ae546-2020>.
- Her, Y.G., Lusher, W.R., & Migliaccio, K.W. (2018). How likely is a 100-year rainfall event during the next ten years? AE523, 3/2018. *Agricultural and Biological Engineering*, 2018(2), 1-4. <http://doi.org/10.32473/edis-ae523-2018>.
- Intergovernmental Panel on Climate Change – IPCC. (2021). *Climate Change 2021: The Physical Science Basis. Contribution of Working Group I to the Sixth Assessment Report of the Intergovernmental Panel on Climate Change*. IPCC.
- Knutson, T.R., & Zeng, F. (2018). Model assessment of observed precipitation trends over land regions: detectable human influences and potential sources of uncertainty. *Journal of Climate*, 31(6), 2143-2162.
- Miller, D.E., & Gardner, W.H. (1962). Water infiltration into stratified soil. *Soil Science Society of America Journal*, 26(2), 115-119.
- Mishra, V., Bhatia, U., & Tiwari, A.D. (2020a). Bias-corrected climate projections for South Asia from coupled model intercomparison project-6. *Scientific Data*, 7(1), 338. PMID:33046709. <http://doi.org/10.1038/s41597-020-00681-1>.
- Nguyen, K.A., & Chen, W. (2021). DEM-and GIS-based analysis of soil erosion depth using machine learning. *ISPRS International Journal of Geo-Information*, 10(7), 452.
- O’Gorman, P.A. (2015). Precipitation extremes under climate change. *Current Climate Change Reports*, 1(2), 49-59. PMID:26312211. <http://doi.org/10.1007/s40641-015-0009-3>.
- Oguz, E.A., Benestad, R.E., Parding, K.M., Depina, I., & Thakur, V. (2024). Quantification of climate change impact on rainfall-induced shallow landslide susceptibility: a case study in central Norway. *Georisk: Assessment and Management of Risk for Engineered Systems and Geohazards*, 18(2), 467-490.
- Pai, D.S., Rajeevan, M., Sreejith, O.P., Mukhopadhyay, B., & Satbha, N.S. (2014). Development of a new high spatial resolution (0.25° × 0.25°) Long Period (1901–2010) daily gridded rainfall data set over India and its comparison with existing data sets over the region. *Mausam (New Delhi)*, 65(1), 1-18. <http://doi.org/10.54302/mausam.v65i1.851>.
- Ramachandra, T.V., & Mujumdar, P.P. (2009). Urban floods: case study of Bangalore. *Journal of the National Institute of Disaster Management*, 3(2), 1-98.
- Ramos, R.D. (2001). *Performance of a fiberglass based geocomposite capillary barrier drain* [Doctoral thesis, University of New Mexico]. University of New Mexico.
- Stormont, J.C., Ramos, R., & Henry, K.S. (2001). Geocomposite capillary barrier drain system with fiberglass transport layer. *Transportation Research Record: Journal of the Transportation Research Board*, 1772(1), 131-136.
- Van Genuchten, M.T. (1980). A closed-form equation for predicting the hydraulic conductivity of unsaturated soils. *Soil Science Society of America Journal*, 44(5), 892-898. <https://doi.org/10.2136/sssaj1980.03615995004400050002x>.
- Westra, S., Fowler, H.J., Evans, J.P., Alexander, L.V., Berg, P., Johnson, F., Kendon, E.J., Lenderink, G., & Roberts, N.M. (2014). Future changes to the intensity and frequency of short-duration extreme rainfall. *Reviews of Geophysics*, 52(3), 522-555.
- Zornberg, J.G., & Mitchell, J.K. (1994). Reinforced soil structures with geosynthetics. *Journal of Geotechnical Engineering*, 120(7), 1155-1176.